Mannheimia haemolytica Leukotoxin Binds to Lipid Rafts in Bovine Lymphoblastoid Cells and Is Internalized in a Dynamin-2- and Clathrin-Dependent Manner[∇]

Dhammika N. Atapattu and Charles J. Czuprynski*

Department of Pathobiological Sciences, University of Wisconsin-Madison, Madison, Wisconsin

Mannheimia haemolytica is the principal bacterial pathogen of the bovine respiratory disease complex. Its most important virulence factor is a leukotoxin (LKT), which is a member of the RTX family of exotoxins produced by many gram-negative bacteria. Previous studies demonstrated that LKT binds to the β_2-integrin LFA-1 (CD11a/CD18) on bovine leukocytes, resulting in cell death. In this study, we demonstrated that depletion of lipid rafts significantly decreases LKT-induced bovine lymphoblastoid cell (BL-3) death. After binding to BL-3 cells, some of the LKT relocated to lipid rafts in an LFA-1-independent manner. We hypothesized that after binding to LFA-1 on BL-3 cells, LKT moves to lipid rafts and clathrin-coated pits via a dynamic process that results in LKT internalization and cytotoxicity. Knocking down dynamin-2 by small interfering RNA reduced both LKT internalization and cytotoxicity. Similarly, expression of dominant negative Eps15 protein expression, which is required for clathrin coat formation, reduced LKT internalization and LKT-mediated cytotoxicity to BL-3 cells. Finally, we demonstrated that inhibiting actin polymerization reduced both LKT internalization and LKT-mediated cytotoxicity. These results suggest that both lipid rafts and clathrin-mediated mechanisms are important for LKT internalization and cytotoxicity in BL-3 cells and illustrate the complex nature of LKT internalization by the cytoskeletal network.

Mannheimia haemolytica is the principal bacterial agent responsible for the bovine respiratory disease complex (50). *M. haemolytica* produces a leukotoxin (LKT) that is considered its most important virulence factor. The LKT belongs to the RTX (repeats in toxin) family of toxins that contain glycine-rich repeats in the primary structure and are produced by a variety of gram-negative bacteria (47). LKT binds to the β_2-integrin LFA-1 (CD11a/CD18) on bovine leukocytes, resulting in apoptosis or cytolysis of bovine cells (2, 25, 32). This response is contrary to the usual outcome of cell signaling via CD11a/CD18, which generally leads to cell activation and survival rather than cell death (11, 24).

It has been shown that upon stimulation, LFA-1 receptors in human neutrophils associate in detergent-resistant membrane microdomains called lipid rafts (14). Lipid rafts are cholesterol- and sphingolipid-enriched membrane structures that are approximately 50 to 100 nm in diameter (39). Coalescence of lipid rafts can result in membrane domains up to 400 nm in diameter that involve up to 30 to 50% of the cell surface, depending on the cell type (22, 42). Lipid rafts have been implicated in several important cellular functions, such as internalization of receptors and their ligands, signal transduction, and cholesterol transport. The relationship between membrane receptors and lipid rafts is highly variable. For example, epidermal growth factor and β_2 adrenergic receptors move away from lipid rafts following receptor activation. In

contrast, insulin and angiotensin II receptors move into lipid rafts following ligand binding, and nerve growth factor and platelet growth factor receptors do not associate with lipid rafts (7, 23).

Numerous bacterial toxins, bacteria, viruses, and parasites use lipid rafts and raft-associated caveolae to bind to cells and be internalized. Examples include *Vibrio cholerae* toxin, *Staphylococcus aureus* α-hemolysin, aerolysin, diphtheria toxin, *Salmonella enterica* serovar Typhimurium, *Shigella flexneri*, *Brucella* species, echovirus 1, and simian virus 40 (34, 41). Alternatively, some bacterial toxins, such as *Pseudomonas* exotoxin A, *V. cholerae* toxin, and anthrax toxin, target the clathrin-mediated endocytic pathway for their internalization (21, 36). One protein common to both the clathrin- and caveola-mediated endocytic pathways is dynamin, a large GTPase that is responsible for budding of clathrin-coated pits and for clipping the neck of caveolae from the cell membrane (37, 38). The three mammalian forms of dynamin (dynamin-1, dynamin-2, and dynamin-3) are generally localized in the plasma membrane, trans-Golgi network, and endosomes, respectively (6, 45).

In this study, we hypothesize that *M. haemolytica* LKT binds to lipid rafts and clathrin-coated pits, followed by internalization into bovine lymphoblastoid (BL-3) cells. We show here that after binding to LFA-1, LKT relocates to lipid rafts in an LFA-1 independent manner. This results in asymmetrical aggregation of lipid rafts on cells. Raft aggregation and internalization of LKT lead to dynamin-, clathrin-, and actin-dependent cytotoxicity of BL-3 cells. These data demonstrate the complex participation of the cytoskeleton in LKT-mediated death of BL-3 cells.

---

* Corresponding author. Mailing address: Department of Pathobiological Sciences, University of Wisconsin, 2015, Linden Drive, West, Madison, WI 53706. Phone and fax: (608) 262-8102. E-mail: czuprync @svm.vetmed.wisc.edu.

MATERIALS AND METHODS

LKT production and purification. Crude LKT was prepared and purified from logarithmic-growth-phase culture filtrates as described previously (3). One unit of LKT activity was defined as the LKT dilution causing 50% killing of 10^6 BL-3 cells when they were incubated at 37°C for 1 h, as determined by trypan blue exclusion. LKT was stored at −80°C until it was used. Culture filtrate from an *lktC* mutant of *M. haemolytica* (SH 1562) that produces an LKT protein with no biological activity was prepared in a manner similar to that used to prepare culture filtrate from wild-type *M. haemolytica* strain A1 (generously provided by S. K. Highlander, Houston, TX).

Cell line and cell culture. BL-3 cells were used as a target for all cytotoxicity experiments in this study (kindly provided by Ronald Schultz, Madison, WI). These nonadherent cells were grown at 37°C in the presence of 5% CO_2 in RPMI medium supplemented with 10% fetal bovine serum (Gibco BRL, Burlington, VT).

LKT cytotoxicity assays. BL-3 cells (10^6 cells per ml) were washed, resuspended in antibiotic-free RPMI medium, and incubated at 37°C with 0.2 or 0.5 U of LKT for the indicated time periods. Cell metabolism was quantified using the Cell Titer 96 AQ one-assay system (Promega Corporation, Madison, WI). The optical density of the reaction mixture was measured at 450 nm using an automated enzyme-linked immunosorbent assay reader (Mini plate EL 312; BIO TEK Instruments Inc., Winooski, VT).

Antibodies and fluorescent probes. A neutralizing monoclonal antibody (MAb) against LKT (MM601) was a generous gift from S. K. Srikumaran (Washington State University, Pullman). Anti-LFA-1 MAb (VMRD, Pullman, WA), anti-flotillin antibody (BD Bioscience, San Jose, CA), anti-dynamin-2 MAb (US Biologicals, Swampscott, MA), rhodamine-conjugated cholera toxin subunit B (CTB-Rho) (Molecular Probes, Carlsbad, CA), and anti-clathrin heavy chain MAb clone X22 or anti-clathrin light chain MAb clone CON.1 (Calbiochem, San Diego, CA, and Lab Vision, Fremont, CA) were used in this study. Rhodamine-labeled transferrin (kindly provided by Linda Schuler, Madison, WI) was used to determine clathrin-mediated internalization in BL-3 cells.

Lipid raft depletion and sequestration. To deplete lipid rafts, BL-3 cells were incubated with serum-free RPMI medium containing 5 mM methyl-β-cyclodextrin (MCD) at 37°C for 30 min. To reconstitute cholesterol in MCD-treated BL-3 cells, the cells were incubated with 10 mM MCD-cholesterol (Sigma Chemicals, St. Louis, MO) in RPMI medium for 30 min at 25°C (18). Raft sequestration was achieved by treating BL-3 cells with filipin (4.5 µg/ml) for 30 min at 37°C.

Dynamin-2 knockdown. Dynamin-2 in BL-3 cells was knocked down with a small interfering RNA (siRNA) designed for the sequence 5′-GGGATGTCCT GGAGAACAA-3′, using the T7 RiboMAX Express RNA interference system (Promega Corporation, Madison, WI). BL-3 cells were transfected with siRNA using the X-treme transfection reagent (Roche, Nutley, NJ) for 6 h, followed by further incubation for 72 h at 37°C. Transfected BL-3 cells were used for cytotoxicity and immunofluorescence studies. Cells transfected with a scrambled siRNA (5′-GCCCTGTTCTATAAATATC-3′) served as a negative control. The reduction in dynamin-2 mRNA knockdown was assessed by an endpoint reverse transcription-PCR assay (with primers F [GGG AAC CTC TGA CCT CTC CAA] and R [CTG GTG CTG ATG TCC CCA AT]) and with immunoblotting.

Clathrin coat inhibition. Clathrin coat formation was inhibited using dominant negative Eps15 plasmid constructs (D111); control cells were incubated with a control plasmid (ΔD111). Both plasmids were generous gifts from Linda Schuler (Madison, WI). Plasmids were transfected into BL-3 cells by incubation for 6 h at 37°C with the FuGENE HD transfection reagent according to the protocol supplied with the reagent (Roche, Nutley, NJ).

Chemical inhibition of clathrin internalization was achieved by K^+ depletion. Briefly, cells were incubated three times for 10 min at 37°C in isotonic K^+-free depletion buffer (140 mM NaCl, 20 mM HEPES-NaOH [pH 7.4], 1 mM $CaCl_2$, 1 mM $MgCl_2$, 1 mg/ml glucose, 0.5% bovine serum albumin). Potassium-depleted BL-3 cells were incubated with LKT or rhodamine-labeled transferrin (a generous gift from Linda Schuler, Madison, WI). In some experiments actin depolymerization was achieved by incubating BL-3 cells in RPMI medium with cytochalasin D (2 µg/ml; Sigma) for 1 h at 37°C.

Transferrin internalization studies. To demonstrate inhibition of clathrin internalization, BL-3 cells were depleted of K^+ by incubation at 4°C for 1 h in K^+-free buffer. Control cells were incubated in normal RPMI medium or in K^+-replete buffer. The cells were then incubated with rhodamine-conjugated transferrin (30 µg/ml) or LKT (0.5 U) for 60 min at 37°C and visualized by fluorescent microscopy.

Staining for cytoskeletal actin with phalloidin-FITC. BL-3 cells were stained with phalloidin-fluorescein isothiocyanate (FITC) according to the protocol provided by Molecular Probes (protocol MP00352). Briefly, BL-3 cells were fixed with 2% paraformaldehyde for 10 min, washed three times with phosphate-buffered saline (PBS), and permeabilized with cold acetone for 10 min. Cells were washed three times with PBS and stained with 20 µM phalloidin-FITC for 20 min at 25°C. Following this the cells were washed three times with PBS and visualized by fluorescent microscopy at an emission wavelength of 480 nm.

Detergent extraction and flotation of lipid rafts. Detergent extraction and flotation of BL-3 cell membranes were performed using a slight modification of a previously described method (30). Briefly, 10^6 BL-3 cells were incubated with 0.5 U of LKT for 30 min at 37°C. The cells were washed three times with PBS and lysed using a mechanical homogenizer, and the lysate was incubated on ice for 30 min in TNE buffer (25 mM Tris-HCl [pH 7.4], 150 mM NaCl, 5 mM EDTA, 1 mM dithiothreitol, protease inhibitor mixture, 1% Triton X-100). Samples were mixed with 40% Optiprep (Nycomed, Altana Inc., New Jersey) and overlaid with 30, 20, 10, and 0% Optiprep to obtain a discontinuous gradient. Samples were then centrifuged at 55,000 rpm in a TLS 55 rotor (Beckman, Fullerton, CA) for 4 h at 4°C. Five fractions were collected from the top to bottom of the tube (designated fractions 1 to 5 from the top to the bottom of the tube). Proteins were precipitated with a chloroform-methanol extraction method and analyzed by Western immunoblotting (48).

Raft patching, clathrin staining, and immunofluorescence confocal microscopy. BL-3 cells were incubated with 0.5 U of LKT for 30 min, washed three times with PBS, and fixed with 2% paraformaldehyde for 10 min at 25°C. Cells were washed three times with PBS and incubated with CTB-Rho for 1 h at 25°C, which was followed by incubation with anti-LKT-FITC for 1 h. Cells were washed three times with PBS and examined using laser confocal microscopy. Clathrin staining was done in a similar manner using anti-clathrin heavy chain MAb. Images were analyzed with Image J software (NIH; http://rsb.info.nih.gov/ij).

Determination of LKT internalization by flow cytometry. BL-3 cells were incubated with 0.5 U of LKT for the indicated times. Cells were washed three times with PBS and fixed with 2% paraformaldehyde for 10 min at 25°C. Some samples were permeabilized with 1% Triton X-100 for 15 min. Cells were then stained with anti-LKT MAb (MM601), followed by FITC-labeled anti-mouse immunoglobulin G (IgG). Flow cytometric analysis was performed with both groups of cells (FACScan; Becton Dickinson, Franklin Lakes, NJ), and the cell population of interest was gated on the basis of forward- and side-scatter light characteristics. The fluorescent intensity of this population was determined and used for the analysis. Heat-inactivated LKT (inactivated by heating at 100°C for 10 min) and *M. haemolytica* producing a biologically inactive *lktC* mutant toxin were used as controls (data not shown).

Statistical analysis. Group means were compared by analysis of variance, followed by the Tukey-Kramer pairwise comparison test, using the Instat statistical package (GraphPad, San Diego, CA). The level of statistical significance was set at $P < 0.05$.

RESULTS

Lipid raft depletion inhibits LKT-mediated cytotoxicity. We first investigated the role of lipid rafts in LKT-mediated cytotoxicity by depleting and sequestrating cholesterol in BL-3 cells using MCD and filipin, respectively. We observed 57 and 50% reductions in cytotoxicity following MCD and filipin treatment, respectively. Cholesterol reconstitution of MCD-treated BL-3 cells restored LKT-mediated cytotoxicity to control levels (Fig. 1).

LKT colocalizes with lipid rafts and clathrin in BL-3 cells. Next we used discontinuous Optiprep gradient ultracentrifugation to fractionate lipid raft and nonraft membrane fractions from LKT-treated BL-3 cells. LKT was detected by immunoblot analysis of the lipid raft samples recovered from the less dense fractions of the Optiprep gradient. As determined by densitometry, approximately 47% of the LKT was associated with the lipid raft fraction. A small amount of LKT (4%) colocalized with LFA-1, and the remainder associated with neither LFA-1 nor raft fractions (Fig. 2). In contrast, 98% of the LKT was found in the bottom fraction of the gradient when we used membrane lysates from cholesterol-depleted BL-3 cells (MCD treated) that lacked lipid rafts (Fig. 2A). The relatively small portion of LKT associated with LFA-1 suggests
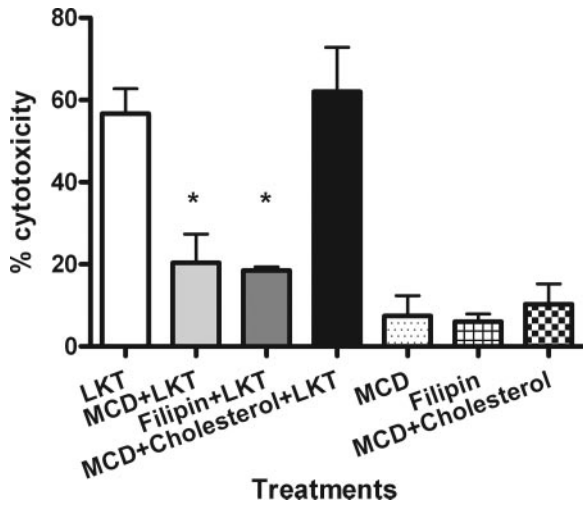
FIG. 1. Depletion and sequestration of lipid rafts in BL-3 cells inhibit LKT-mediated cytotoxicity. BL-3 cells were pretreated for 30 min at 37°C with either 5 mM MCD (to deplete cholesterol) or 4.5 μg/ml filipin (to sequester lipid rafts). Cells were then incubated with LKT (0.5 U) for 1 h. Cell viability was measured in a cytotoxicity assay as described in Materials and Methods. Some MCD-treated BL-3 cells were incubated with MCD-10 mM cholesterol (to reconstitute lipid rafts) before exposure to LKT. BL-3 cells incubated with MCD, filipin, or MCD-cholesterol alone were included as controls. Data are expressed as means and standard errors of the means of three separate experiments. An asterisk indicates that the *P* value is <0.05 for a comparison with BL-3 cells exposed to LKT alone.

that binding of LKT to LFA-1 is a transient process. LKT not associated with either lipid rafts or LFA-1 was found in the higher-density membrane fraction, associated with clathrin (Fig. 2C) (23).

Unclustered lipid rafts are too small to be visualized by light microscopy (51). Once stimulated, they form aggregates up to 400 nm in diameter that enable them to be visualized by fluorescent tagging of raft-associated glycosylphosphatidylinisotol-anchored proteins. Using CTB-Rho (which binds to a GM1 ganglioside receptor) as a marker for lipid rafts, we observed colocalization of LKT with lipid rafts on BL-3 cells by confocal microscopy. Confocal micrographs revealed a focal distribution of LKT on lipid rafts, with raft aggregation and localization visible at one pole of the cell. However, not all cells stained positive for either LKT or CTB-Rho, which may indicate that there is heterogeneity of ganglioside receptor expression on the surface of BL-3 cells (Fig. 3). Staining for clathrin-coated pits (i.e., anti-clathrin heavy chain antibodies) demonstrated colocalization of clathrin with LKT in BL-3 cells.

LKT is internalized into BL-3 cells. Binding of proteins to lipid rafts may result in trafficking of proteins into the cell. Therefore, we next investigated whether LKT remains on the cell surface of BL-3 cells. Surface staining for LKT on BL-3 cells began to decrease by about 30 min, while the total signal for LKT (determined by staining permeabilized BL-3 cells) remained unchanged (Fig. 4). These findings suggest that once bound to the cell, LKT is internalized and remains within the cell for at least 1 h.

LKT-mediated cytotoxicity and internalization is dynamin, clathrin, and actin dependent. Next we investigated possible pathways by which LKT might be internalized into BL-3 cells. Using siRNA to knock down dynamin-2 expression, we reduced LKT-mediated cytotoxicity by approximately one-half the value for control LKT-treated BL-3 cells. Using FITC-conjugated anti-LKT MAb and fluorescent microscopy, we
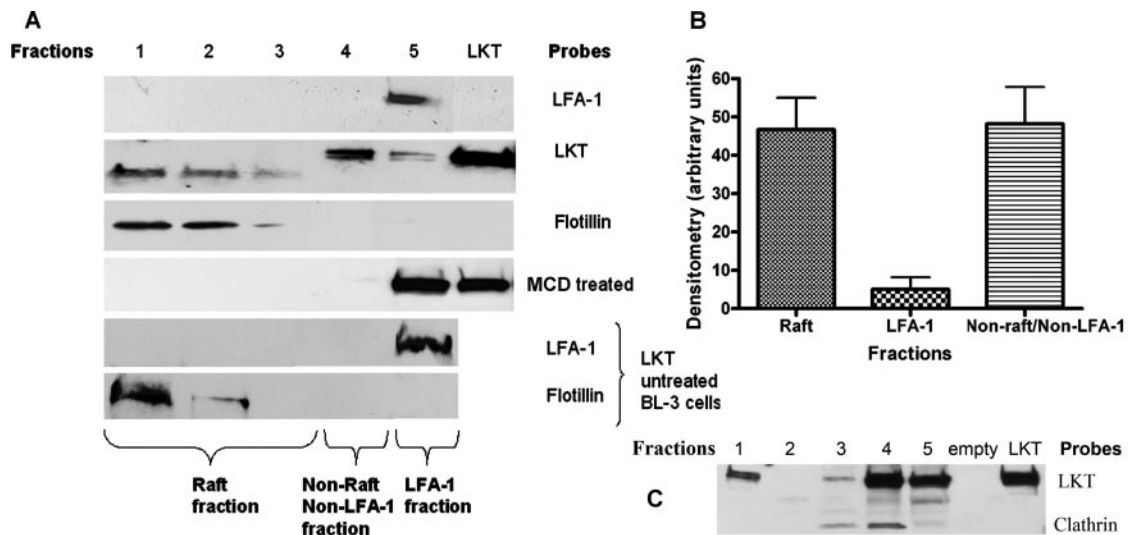

FIG. 2. LKT associates with detergent-resistant membrane fractions (lipid rafts) in BL-3 cells. A total of 10^6 BL-3 cells were incubated with LKT (0.5 U) for 30 min at 37°C and then lysed with TNE buffer. The lysates were centrifuged at $10,000 \times g$ for 15 min. Detergent-resistant membrane fractions were isolated on Optiprep discontinuous gradients, and five fractions were collected from the top to the bottom (designated fractions 1 to 5). In panel A, protein was extracted from each fraction, and Western immunoblotting was performed for LKT, LFA-1, and flotillin. BL-3 cells depleted of cholesterol by MCD treatment and lipid raft fractions from non-LKT-treated BL-3 cells were included as controls and probed with anti-LFA-1 and anti-flotillin antibodies. In panel C, protein was extracted from each fraction, and Western immunoblotting was performed for LKT and clathrin light chain. This allowed us to characterize LFA-1 and LKT in raft and nonraft fractions. In panel B, the intensities of LKT bands in raft and nonraft fractions in panel A were quantified using LabWorks analysis software and are expressed as means and standard errors of the means of three separate experiments.
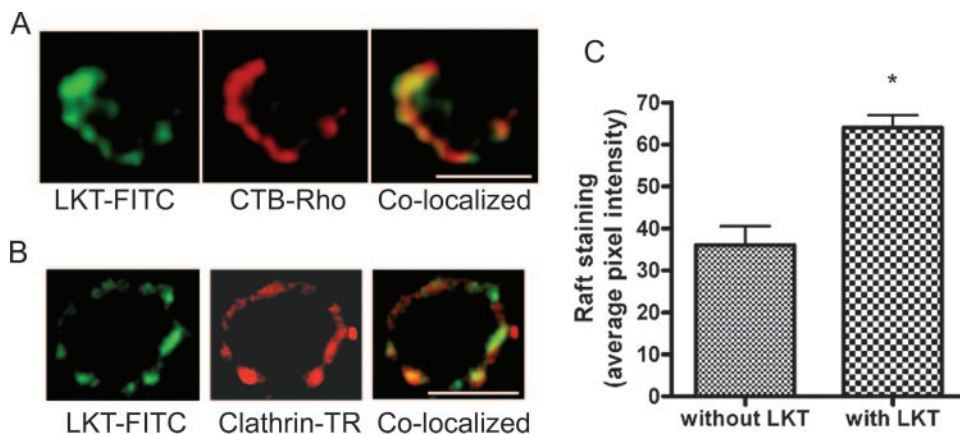
FIG. 3. LKT colocalizes with lipid rafts and clathrin pits on BL-3 cells. A total of 10^6 BL-3 cells were incubated with LKT (0.5 U) for 30 min at 37°C. Cells were then fixed with 2% paraformaldehyde for 10 min, blocked with 3% bovine serum albumin for 20 min, and incubated for 1 h at 25°C with FITC-conjugated anti-LKT MAb, CTB-Rho (which binds to GM1 associated with lipid rafts), or Texas Red (TR)-conjugated anti-clathrin heavy chain antibody. Cells were visualized with a confocal microscope. Panel A shows a single cell in which LKT (green) colocalized with lipid rafts (red). Panel B shows colocalization of LKT with clathrin (red). In panel C, the mean lipid raft fluorescence intensities of images from 50 randomly selected cells were quantified for LKT-induced raft aggregation, using Image J software (NIH; http://rsb.info.nih.gov/ij). Bars = 10 μm.

also demonstrated a significant reduction in LKT internalization by siRNA-treated BL-3 cells (Fig. 5).

Dynamin-2 is a membrane scission protein that participates in both lipid raft caveola-dependent and clathrin-dependent vesicle trafficking in cells. We assessed the role of dynamin-2 in LKT-mediated cytotoxicity by several methods. We first addressed the role of the Eps15 protein, which along with the AP-2 adaptor complex forms an integral part of the clathrin-coated pit. To do this, we used a dominant negative Eps15 DIII protein that lacks the Eps15 homology domains and coiled coil regions that are required for the assembly of clathrin pits (4, 5).
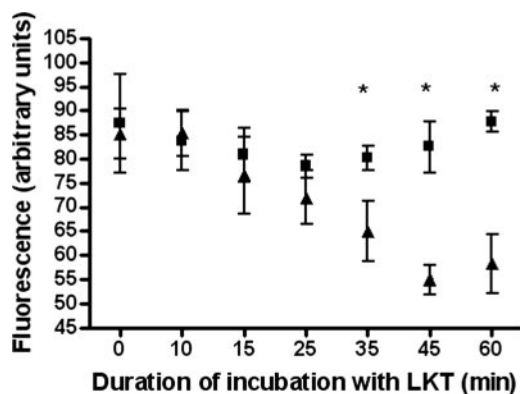

FIG. 4. Surface fluorescence for LKT on BL-3 cells decreased with time, while total fluorescence remained unchanged. A total of 10^6 BL-3 cells were incubated with LKT (0.5 U) for the indicated times (5 to 60 min) at 37°C and then fixed with 2% paraformaldehyde. Fixed BL-3 cells were stained with FITC-conjugated anti-LKT antibody for 60 min at 25°C, and the surface fluorescence was analyzed by flow cytometry (▲). To quantify total fluorescence of cells (■), LKT-treated BL-3 cells were permeabilized with cold acetone (−20°C) for 10 min before labeling with FITC-conjugated anti-LKT antibody. The cells were then analyzed by flow cytometry. Fluorescence is expressed as the means ± standard errors of the means of three separate experiments. An asterisk indicates that the P value is <0.05.

LKT-mediated cytotoxicity was significantly reduced when we inhibited clathrin coat formation and internalization by transfecting BL-3 cells with a plasmid (Eps15 DIII) that expresses a dominant negative Eps15 protein (Fig. 6). Immunofluorescence microscopy confirmed that LKT internalization was also significantly decreased in Eps15 DIII plasmid-transfected cells compared to cells transfected with a control ΔDIII Eps15 plasmid. Inhibition of internalization of transferrin, which is transported exclusively by a clathrin-mediated pathway, confirmed that clathrin coat formation was inhibited in dominant negative Eps15 protein-expressing BL-3 cells. We also used K^+ depletion to investigate clathrin-mediated internalization of LKT. K^+ depletion in BL-3 cells resulted in a 42% reduction in cytotoxicity (Fig. 7) and a significant reduction in LKT internalization, as determined by immunofluorescence microscopy (data not shown).

Finally, we investigated the role of cytoskeletal actin polymerization in LKT internalization. Treating BL-3 cells with the selective inhibitor cytochalasin D reduced LKT-mediated cytotoxicity from 61% (control cells) to 18% (cytochalasin D-treated cells) and similarly reduced internalization of LKT into BL-3 cells (Fig. 8).

DISCUSSION

The observations made in this study, together with other recent reports, demonstrate that the molecular interactions between RTX toxins and their target cells are complex. Originally, the primary mechanism of RTX toxin-induced cytotoxicity was thought to be pore formation in the cytoplasmic membrane. Later studies demonstrated that the *M. haemolytica* LKT binds to LFA-1 (CD11a/CD18) before inducing cell death by apoptosis (3, 10, 20, 25). Binding of LKT to LFA-1 results in phosphorylation of the cytoplasmic tail of CD18 (26). Signaling through β_2-integrins usually transmits a survival signal. These disparate findings suggest that LKT may stimulate a cascade of events that may induce cell death by an uncharac-
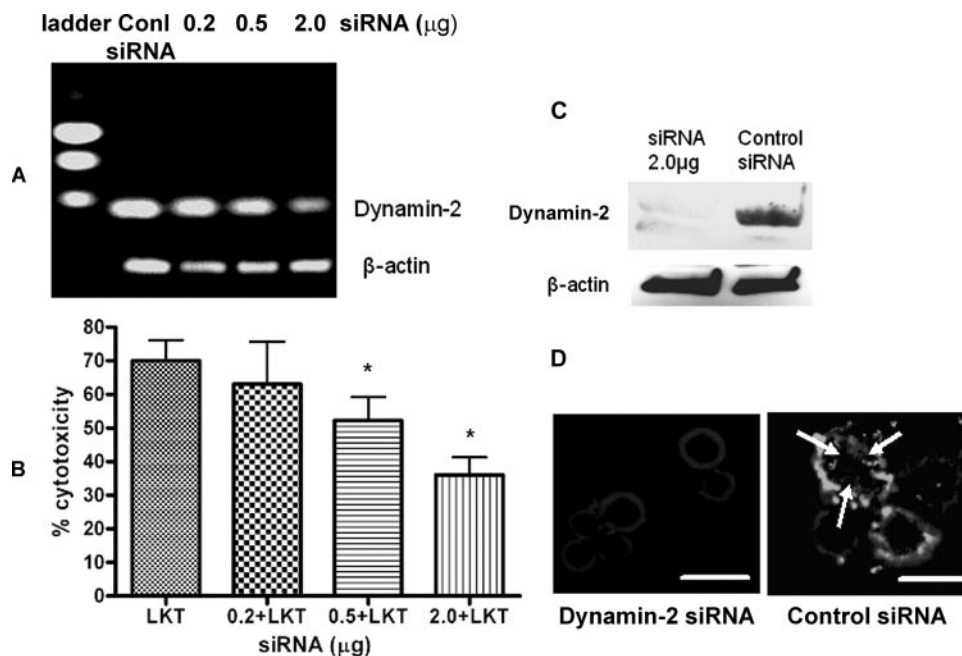
FIG. 5. siRNA knockdown of dynamin-2 reduces LKT-mediated cytotoxicity and internalization in BL-3 cells. Dynamin-2 was knocked down by transfecting BL-3 cells with siRNA (0.2, 0.5, or 2.0 μg) for 6 h, followed by further incubation in RPMI medium with 10% fetal bovine serum for 72 h. Control cells were transfected with a scrambled siRNA sequence for the same time period. To assess the degree of dynamin-2 RNA knockdown, RNA was extracted, and a one-step reverse transcription-PCR assay with dynamin-2-specific primers was performed. In panel A the products were visualized by electrophoresis in a 1% agarose gel. In panel B, dynamin-2 siRNA- or scrambled siRNA-transfected BL-3 cells (10^6) were incubated with LKT (0.5 U) for 1 h, and cytotoxicity was measured as described previously. The data are the means and standard errors of the means of five separate siRNA transfection experiments. An asterisk indicates that the P value is <0.05 for a comparison with the scrambled siRNA control. Panel C shows an immunoblot analysis of dynamin-2 knockdown from BL-3 cells transfected with 2 μg of dynamin-2 siRNA. In panel D, BL-3 cells transfected with dynamin-2 siRNA (2.0 μg) or with scrambled siRNA were fixed, permeabilized with cold acetone, blocked with 3% bovine serum albumin, and incubated with anti-LKT MAb. A goat anti-mouse IgG-Texas Red-conjugated secondary antibody was added, and the LKT signal was visualized by fluorescent microscopy at excitation and emission wavelengths of 595 and 614 nm, respectively. The arrows indicate internalized LKT. Bars = 10 μm. Conl, control.

terized pathway, perhaps in a receptor-independent manner (16, 31). More recently, it has been shown that a related RTX toxin, the hemolysin of *Escherichia coli* (HlyA), can bind to target cells independent of its receptor. The physical properties of the cell membrane have been suggested to play a major role in HlyA-induced cell death (46).

In this study, we demonstrate that early association of LKT with lipid rafts and clathrin-coated pits results in LKT internalization in a dynamin-2- and actin-dependent manner. These events are essential components of the pathway by which LKT induces BL-3 cell death. Recent studies of the *Actinobacillus actinomycetemcomitans* RTX toxin (LTX) showed that it too binds to lipid microdomains in a similar manner (15). In our study, we showed that diminution of lipid rafts by cholesterol depletion significantly reduced LKT-mediated cytotoxicity. Membrane fractionation demonstrated that a substantial proportion of the *M. haemolytica* LKT (~47%) was associated with lipid rafts. However, an estimated 49% of LKT was associated with neither LFA-1 nor the lipid raft-containing membrane fractions. Based on previous reports that clathrin localizes mostly in the denser and lower fractions of an Optiprep density gradient, we suggest that the LKT contained in the cell membrane fraction that lacks rafts or LFA-1 might be associated with clathrin-coated pits (23). LFA-1 was not associated with lipid rafts in either LKT-treated or control BL-3 cells.

Consistent with previous reports, we also demonstrated that lipid raft depletion of BL-3 cells (by MCD treatment) did not alter LFA-1 expression (data not shown) (35). These findings, therefore, suggest that LFA-1 might provide only a temporary docking site for the initial binding of LKT. Once LKT dissociated from LFA-1, the former moved to lipid rafts, while LFA-1 remained in the raft-free cell membrane fraction (Fig. 2). This explanation is consistent with previous observations by Leitinger and Hogg, who found that LFA-1 is excluded from lipid rafts until the cells are stimulated (33). Movement of LFA-1 and associated protein complexes (integrin-associated proteins) to lipid rafts depends on both ligand binding and release of cytoskeletal constraints. There are other examples of bacterial toxins translocating from one protein to another on target cell surfaces. For example, tetanus toxin binds to a receptor complex which consists of polysialogangliosides (GD1b and GT1b) and glycosylphosphatidylinositol-anchored proteins on the neuronal cell surface. Once tetanus toxin binds to GD1b, it dissociates from this receptor and is then internalized via a clathrin-dependent pathway (8). More detailed studies are, however, needed to definitively demonstrate lateral translocation of LKT from LFA-1 to lipid rafts.

Using confocal microscopy, we demonstrated that lipid raft aggregation occurred asymmetrically on the BL-3 cell, at sites where LKT also appeared to accumulate. Interestingly, not all
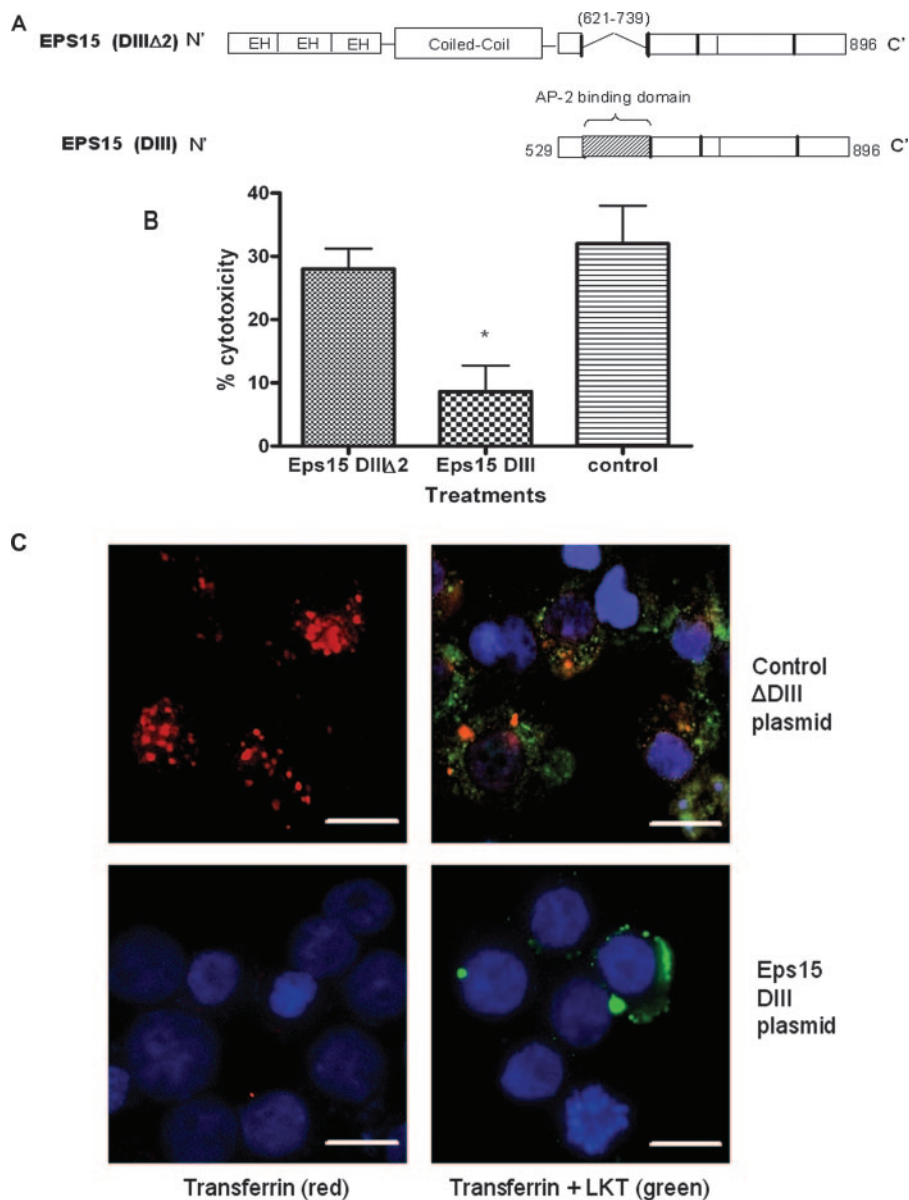
FIG. 6. Expression of a dominant negative Eps15 protein in BL-3 cells inhibits clathrin-dependent internalization of LKT and LKT-mediated cytotoxicity. Panel A is a schematic representation of the dominant negative mutant Eps15 protein (DIII) and the control Eps15 protein (DIIIΔ2) expressed in BL-3 cells. In the Eps15 (DIII) construct, the Eps15 homology domains (EH) and N-terminal coiled coil domains that are required for clathrin coat assembly have been deleted. In panel B, BL-3 cells were transfected with 6 μg of Eps15 DIII or the control Eps15 DIII Δ2 plasmid for 6 h at 37°C and then incubated with LKT (0.2 U) for 1 h at 37°C. Cytotoxicity was measured as described previously. The data are the means and standard errors of the means of three separate experiments. The asterisk indicates that the P value is <0.05. In panel C, BL-3 cells transfected with the Eps15 DIII or Eps15 DIII Δ2 plasmid were stained for cytoplasmic LKT and for transferrin (which is internalized by the clathrin-mediated pathway). BL-3 cells incubated with LKT were fixed, permeabilized, blocked with 3% bovine serum albumin, and incubated with FITC-conjugated anti-LKT MAb and rhodamine-conjugated transferrin. Images were visualized by confocal microscopy. The control plasmid-transfected BL-3 cells demonstrated internalization of transferrin (red) and LKT (green), while the Eps15 DIII plasmid-transfected BL-3 cells showed reduced internalization of LKT and virtually no signal from transferrin. Cells were counterstained with 4′,6′-diamidino-2-phenylindole (DAPI) nuclear stain (blue). The images in panel C show representative cells from three separate experiments that were performed. Bars = 10 μm.

BL-3 cells stained positive for both LKT and lipid rafts (the latter was assessed by CTB-Rho staining). This finding probably reflects the unsynchronized growth of BL-3 cells, which are rapidly multiplying blast cells. Cells at different stages of the cell cycle may express different amounts of membrane proteins and lipid rafts (19). Some recent studies show that the lipid raft marker GM1, which binds CTB, also resides in clathrin-coated pits on the cell surface (28). Internalization of CTB-Rho, therefore, could occur via two possibly independent pathways. This would result in heterogeneous staining for CTB-Rho among the BL-3 cells. Aggregation of lipid rafts and clathrin coats with LKT could be an important early event that facilitates pore formation, LKT internalization, or signaling that leads to cell death.
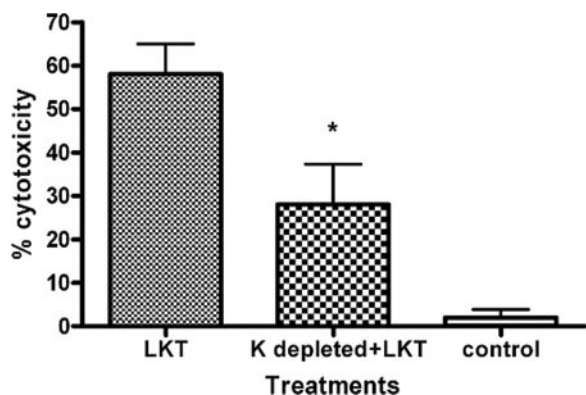
FIG. 7. Potassium depletion in BL-3 cells inhibits LKT-mediated cytotoxicity. BL-3 cells were depleted of K $^+$ by incubation in K$^+$-free buffer for 60 min. Cells were then incubated with LKT, and cytotoxicity was measured. BL-3 cells treated with heat-inactivated LKT and K$^+$-depleted BL-3 cells alone served as controls. The data are the means and standard errors of the means of three separate experiments performed. The asterisk indicates that the _P_ value is <0.05 for a comparison with K$^+$-depleted BL-3 cells. K$^+$-depleted BL-3 cells demonstrated a significant reduction in tranferrin and LKT internalization (data not shown).

FIG. 8. Cytochalasin D treatment inhibits LKT-mediated cytotoxicity and LKT internalization in BL-3 cells. In panel A, β-actin was depleted by treating BL-3 cells with cytochalasin D (Cytochal D) (2 μg/ml) for 60 min. Cells were then incubated with LKT, and cytotoxicity was assessed as described in the text. The data are as the means and standard errors of the means of three separate experiments performed. The asterisk indicates that the _P_ value is <0.05 for a comparison with LKT alone. In panel B, intracellular staining for LKT was performed using an anti-LKT MAb and Texas Red-conjugated anti-mouse IgG. FITC-conjugated phalloidin was added to visualize actin filaments, and BL-3 cells were visualized by fluorescent microscopy. Cytochalasin D-treated cells showed a reduction in LKT internalization (red) and staining for β-actin (green). Cells were counterstained with DAPI nuclear stain (blue). BL-3 cells alone or treated with cytochalasin D were used as controls. Bar = 10 μm.

Binding of protein toxins to lipid rafts could trigger toxin internalization and trafficking of ligand-receptor complexes within cells (21, 49). Internalization of LFA-1 could occur either independent of or in association with lipid rafts (14). Our observation that surface staining for LKT on BL-3 cells decreases with time suggests that once bound to BL-3 cells, LKT molecules are internalized and do not recirculate to the cell surface within 60 min. Because only about 4% of LKT was associated with LFA-1 at any single time point, we infer that LKT internalization is largely LFA-1 independent and perhaps dependent on both lipid raft and nonraft membrane fractions. However, recent studies showed that LFA-1 is internalized and recirculated within peripheral blood neutrophils (14). Thus, we cannot definitively exclude the possibility that a small fraction of LKT trafficked into the BL-3 cells along with LFA-1.

Our investigation provided evidence for the importance of dynamin-2 in lipid raft- and clathrin-mediated LKT internalization. Dynamin-2 is a large GTPase that is responsible for clipping off both caveolae and clathrin vesicles from the cell membrane (45). Our data suggest that dynamin-2 plays a role in LKT internalization, possibly by modulating the cytoskeleton-microtubule network. This in turn could lead to formation of transport vesicles that contain LKT. The role of clathrin in trafficking of other bacterial toxins into the cell is well documented (1, 21). Furthermore, there is now evidence that depletion or sequestration of cholesterol also depletes cells of clathrin-coated pits (44). The close relationship between lipid rafts and clathrin coats makes it difficult to distinguish between these two pathways of protein trafficking (8, 29). Factors that determine whether LKT is transported via one pathway or the other are not yet defined, nor is it certain that these pathways are mutually exclusive. Perhaps the dynamics of LKT movement on the cell membrane determines the pathway by which LKT is internalized into BL-3 cells.

It was interesting to note that knocking down dynamin-2 had approximately the same impact on LKT-mediated cytotoxicity
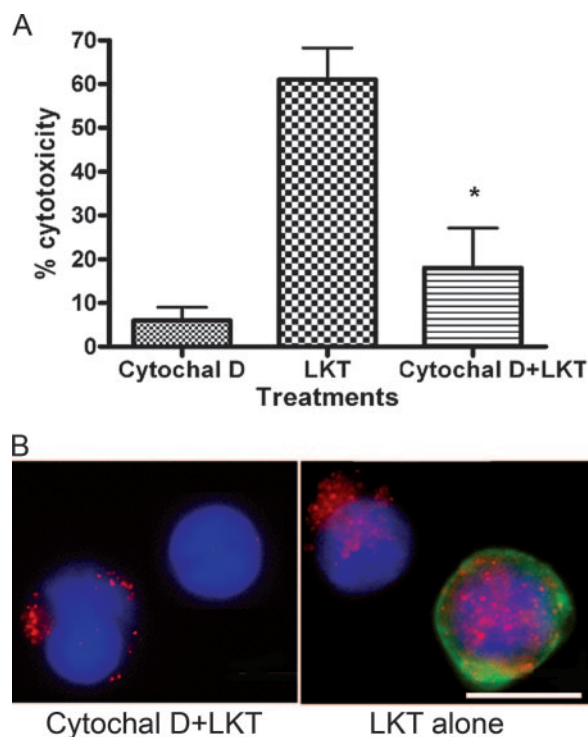
of BL-3 cells (50% reduction in cytotoxicity) as inhibiting clathrin-coated vesicle formation had (42 to 66% reduction in cytotoxicity). Attempts to inhibit both pathways (combined dynamin-2 and clathrin knockdown) failed, due to a high rate of BL-3 cell death. Thus, we cannot exclude the possibility that LKT is internalized via both clathrin- and lipid raft-independent pathways. Furthermore, recent investigations revealed that numerous other mechanisms may be involved in protein trafficking into cells (29). For example, endocytosis in neuronal cells and lymphocytes occurs via lipid rafts that lack caveolae (12, 52). In our study, we were unable to demonstrate the presence of caveolae in BL-3 cells using immunoblotting and immunofluorescence techniques (data not shown). Although this does not completely exclude the possibility of caveolae in BL-3 cells, it seems likely that internalization of LKT is lipid raft associated but independent of caveolae.

An unexpected observation in this study was that LKT binding decreased when BL-3 cells were treated with cytochalasin D or clathrin coat formation was inhibited. As suggested in recent reports, perhaps actin and related cytoskeletal proteins

were responsible for surface clustering or membrane expression of LFA-1 (17, 40). Inhibition of actin polymerization reduced LKT-mediated cytotoxicity and LKT internalization in BL-3 cells. This finding indicates that cytoskeletal proteins play a crucial role in either LKT association with membrane lipid rafts or internalization of LKT-bearing vesicles into BL-3 cells. Actin and talin tethered to the cytoplasmic tail of LFA-1 are responsible for its movement on the cell surface, while β-actin is responsible for the internalization of clathrin-coated vesicles following membrane excision by dynamins (13). Dynamins have been shown to relax the integrin-stress fiber connection, which in turn allows focal adhesion components to disassemble and integrins to be endocytosed or move across the cell membrane (9). Thus, knocking down dynamin would inhibit disassembly of membrane receptor complexes in BL-3 cells, thereby preventing vesicle endocytosis. Inhibition of actin polymerization in BL-3 cells seemed to have an effect on LKT internalization similar to the effect of reduction of dynamin. This observation is consistent with the hypothesis that actin fibers serve two apparently disparate functions in the cell: holding membrane integrins in place and promoting vesicle endocytosis (27, 43).

In summary, the cellular mechanisms by which RTX toxins cause cell damage are complex and intriguing. Our study indicates that after LKT binds to LFA-1, LKT relocation to lipid rafts, raft clustering, clathrin pit formation, and dynamin-2- and actin-dependent internalization of LKT are a series of dynamic events that ultimately lead to death of BL-3 cells. To our knowledge, this is the first report of an RTX toxin which employs lipid rafts and clathrin-coated pits for its internalization and cytotoxicity. Future investigations should identify additional events that are involved in the cytotoxicity of this reported group of toxins.

ACKNOWLEDGMENTS

REFERENCES

1. **Abrami, L., S. Liu, P. Cosson, S. H. Leppla, and F. G. van der Goot.** 2003. Anthrax toxin triggers endocytosis of its receptor via a lipid raft-mediated clathrin-dependent process. J. Cell Biol. **160:**321–328.
2. **Ambagala, T. C., A. P. Ambagala, and S. Srikumaran.** 1999. The leukotoxin of *Pasteurella haemolytica* binds to beta(2) integrins on bovine leukocytes. FEMS Microbiol. Lett. **179:**161–167.
3. **Atapattu, D. N., and C. J. Czuprynski.** 2005. *Mannheimia haemolytica* leukotoxin induces apoptosis of bovine lymphoblastoid cells (BL-3) via a caspase-9-dependent mitochondrial pathway. Infect. Immun. **73:**5504–5513.
4. **Benmerah, A., M. Bayrou, N. Cerf-Bensussan, and A. Dautry-Varsat.** 1999. Inhibition of clathrin-coated pit assembly by an Eps15 mutant. J. Cell Sci. **112:**1303–1311.
5. **Benmerah, A., C. Lamaze, B. Begue, S. L. Schmid, A. Dautry-Varsat, and N. Cerf-Bensussan.** 1998. AP-2/Eps15 interaction is required for receptor-mediated endocytosis. J. Cell Biol. **140:**1055–1062.
6. **Cao, H., H. M. Thompson, E. W. Krueger, and M. A. McNiven.** 2000. Disruption of Golgi structure and function in mammalian cells expressing a mutant dynamin. J. Cell Sci. **113:**1993–2002.
7. **Czech, M. P.** 2000. Lipid rafts and insulin action. Nature **407:**147–148.
8. **Deinhardt, K., O. Berninghausen, H. J. Willison, C. R. Hopkins, and G. Schiavo.** 2006. Tetanus toxin is internalized by a sequential clathrin-dependent mechanism initiated within lipid microdomains and independent of epsin1. J. Cell Biol. **174:**459–471.
9. **del Pozo, M. A., N. Balasubramanian, N. B. Alderson, W. B. Kiosses, A. Grande-Garcia, R. G. Anderson, and M. A. Schwartz.** 2005. Phospho-caveolin-1 mediates integrin-regulated membrane domain internalization. Nat. Cell Biol. **7:**901–908.
10. **Deshpande, M. S., T. C. Ambagala, A. P. Ambagala, M. E. Kehrli, Jr., and S. Srikumaran.** 2002. Bovine CD18 is necessary and sufficient to mediate *Mannheimia* (*Pasteurella*) *haemolytica* leukotoxin-induced cytolysis. Infect. Immun. **70:**5058–5064.
11. **Devine, L., S. L. Lightman, and J. Greenwood.** 1996. Role of LFA-1, ICAM-1, VLA-4 and VCAM-1 in lymphocyte migration across retinal pigment epithelial monolayers in vitro. Immunology **88:**456–462.
12. **Dupre, S., and R. Haguenauer-Tsapis.** 2003. Raft partitioning of the yeast uracil permease during trafficking along the endocytic pathway. Traffic **4:**83–96.
13. **Dykstra, M., A. Cherukuri, H. W. Sohn, S. J. Tzeng, and S. K. Pierce.** 2003. Location is everything: lipid rafts and immune cell signaling. Annu. Rev. Immunol. **21:**457–481.
14. **Fabbri, M., S. Di Meglio, M. C. Gagliani, E. Consonni, R. Molteni, J. R. Bender, C. Tacchetti, and R. Pardi.** 2005. Dynamic partitioning into lipid rafts controls the endo-exocytic cycle of the alphaL/beta2 integrin, LFA-1, during leukocyte chemotaxis. Mol. Biol. Cell **16:**5793–5803.
15. **Fong, K. P., C. M. Pacheco, L. L. Otis, S. Baranwal, I. R. Kieba, G. Harrison, E. V. Hersh, K. Boesze-Battaglia, and E. T. Lally.** 2006. *Actinobacillus actinomycetemcomitans* leukotoxin requires lipid microdomains for target cell cytotoxicity. Cell. Microbiol. **8:**1753–1767.
16. **Frey, J., and P. Kuhnert.** 2002. RTX toxins in Pasteurellaceae. Int. J. Med. Microbiol. **292:**149–158.
17. **Galbraith, C. G., K. M. Yamada, and J. A. Galbraith.** 2007. Polymerizing actin fibers position integrins primed to probe for adhesion sites. Science **315:**992–995.
18. **Giesemann, T., T. Jank, R. Gerhard, E. Maier, I. Just, R. Benz, and K. Aktories.** 2006. Cholesterol-dependent pore formation of *Clostridium difficile* toxin A. J. Biol. Chem. **281:**10808–10815.
19. **Gniadecki, R., and B. Bang.** 2003. Flotillas of lipid rafts in transit amplifying cell-like keratinocytes. J. Investig. Dermatol. **121:**522–528.
20. **Gopinath, R. S., T. C. Ambagala, M. S. Deshpande, R. O. Donis, and S. Srikumaran.** 2005. *Mannheimia* (*Pasteurella*) *haemolytica* leukotoxin binding domain lies within amino acids 1 to 291 of bovine CD18. Infect. Immun. **73:**6179–6182.
21. **Hansen, G. H., S. M. Dalskov, C. R. Rasmussen, L. Immerdal, L. L. Niels-Christiansen, and E. M. Danielsen.** 2005. Cholera toxin entry into pig enterocytes occurs via a lipid raft- and clathrin-dependent mechanism. Biochemistry **44:**873–882.
22. **Hoekstra, D., O. Maier, J. M. van der Wouden, T. A. Slimane, and I. S. C. van Ijzendoom.** 2003. Membrane dynamics and cell polarity: the role of sphingolipids. J. Lipid Res. **44:**869–877.
23. **Huo, H., X. Guo, S. Hong, M. Jiang, X. Liu, and K. Liao.** 2003. Lipid rafts/caveolae are essential for insulin-like growth factor-1 receptor signaling during 3T3-L1 preadipocyte differentiation induction. J. Biol. Chem. **278:**11561–11569.
24. **Inoue, S., A. Nakao, W. Kishimoto, H. Murakami, A. Harada, T. Nonami, and H. Takagi.** 1996. LFA-1 (CD11a/CD18) and ICAM-1 (CD54) antibodies attenuate superoxide anion release from polymorphonuclear leukocytes in rats with experimental acute pancreatitis. Pancreas **12:**183–188.
25. **Jeyaseelan, S., S. L. Hsuan, M. S. Kannan, B. Walcheck, J. F. Wang, M. E. Kehrli, E. T. Lally, G. C. Sieck, and S. K. Maheswaran.** 2000. Lymphocyte function-associated antigen 1 is a receptor for *Pasteurella haemolytica* leukotoxin in bovine leukocytes. Infect. Immun. **68:**72–79.
26. **Jeyaseelan, S., M. S. Kannan, R. E. Briggs, P. Thumbikat, and S. K. Maheswaran.** 2001. *Mannheimia haemolytica* leukotoxin activates a nonreceptor tyrosine kinase signaling cascade in bovine leukocytes, which induces biological effects. Infect. Immun. **69:**6131–6139.
27. **Kaksonen, M., C. P. Toret, and D. G. Drubin.** 2006. Harnessing actin dynamics for clathrin-mediated endocytosis. Nat. Rev. Mol. Cell. Biol. **7:**404–414.
28. **Kirkham, M., A. Fujita, R. Chadda, S. J. Nixon, T. V. Kurzchalia, D. K. Sharma, R. E. Pagano, J. F. Hancock, S. Mayor, and R. G. Parton.** 2005. Ultrastructural identification of uncoated caveolin-independent early endocytic vehicles. J. Cell Biol. **168:**465–476.
29. **Kirkham, M., and R. G. Parton.** 2005. Clathrin-independent endocytosis: new insights into caveolae and non-caveolar lipid raft carriers. Biochim. Biophys. Acta **1746:**349–363.
30. **Lafont, F., and K. Simons.** 2001. Raft-partitioning of the ubiquitin ligases Cbl and Nedd4 upon IgE-triggered cell signaling. Proc. Natl. Acad. Sci. USA **98:**3180–3184.
31. **Lally, E. T., R. B. Hill, I. R. Kieba, and J. Korostoff.** 1999. The interaction between RTX toxins and target cells. Trends Microbiol. **7:**356–361.
32. **Lally, E. T., I. R. Kieba, A. Sato, C. L. Green, J. Rosenbloom, J. Korostoff, J. F. Wang, B. J. Shenker, S. Ortlepp, M. K. Robinson, and P. C. Billings.**

1997. RTX toxins recognize a beta-2 integrin on the surface of human target cells. J. Biol. Chem. **272:**30463–30469.

33. **Leitinger, B., and N. Hogg.** 2002. The involvement of lipid rafts in the regulation of integrin function. J. Cell Sci. **115:**963–972.

34. **Manes, S., G. del Real, and A. C. Martinez.** 2003. Pathogens: raft hijackers. Nat. Rev. Immunol. **3:**557–568.

35. **Marwali, M. R., M. A. MacLeod, D. N. Muzia, and F. Takei.** 2004. Lipid rafts mediate association of LFA-1 and CD3 and formation of the immunological synapse of CTL. J. Immunol. **173:**2960–2967.

36. **Morris, R. E., and C. B. Saelinger.** 1983. Diphtheria toxin does not enter resistant cells by receptor-mediated endocytosis. Infect. Immun. **42:**812–817.

37. **Muro, S., R. Wiewrodt, A. Thomas, L. Koniaris, S. M. Albelda, V. R. Muzykantov, and M. Koval.** 2003. A novel endocytic pathway induced by clustering endothelial ICAM-1 or PECAM-1. J. Cell Sci. **116:**1599–1609.

38. **Nichols, B.** 2003. Caveosomes and endocytosis of lipid rafts. J. Cell Sci. **116:**4707–4714.

39. **Ostrom, R. S., and P. A. Insel.** 2006. Methods for the study of signaling molecules in membrane lipid rafts and caveolae. Methods Mol. Biol **332:** 181–191.

40. **Palazzo, A. F., C. H. Eng, D. D. Schlaepfer, E. E. Marcantonio, and G. G. Gundersen.** 2004. Localized stabilization of microtubules by integrin- and FAK-facilitated Rho signaling. Science **303:**836–839.

41. **Palmer, M.** 2004. Cholesterol and the activity of bacterial toxins. FEMS Microbiol. Lett. **238:**281–289.

42. **Pike, L. J.** 2003. Lipid rafts: bringing order to chaos. J. Lipid Res. **44:**655–667.

43. **Smythe, E., and K. R. Ayscough.** 2006. Actin regulation in endocytosis. J. Cell Sci. **119:**4589–4598.

44. **Subtil, A., I. Gaidarov, K. Kobylarz, M. A. Lampson, J. H. Keen, and T. E. McGraw.** 1999. Acute cholesterol depletion inhibits clathrin-coated pit budding. Proc. Natl. Acad. Sci. USA **96:**6775–6780.

45. **Urrutia, R., J. R. Henley, T. Cook, and M. A. McNiven.** 1997. The dynamins: redundant or distinct functions for an expanding family of related GTPases? Proc. Natl. Acad. Sci. USA **94:**377–384.

46. **Valeva, A., I. Walev, H. Kemmer, S. Weis, I. Siegel, F. Boukhallouk, T. M. Wassenaar, T. Chavakis, and S. Bhakdi.** 2005. Binding of *Escherichia coli* hemolysin and activation of the target cells is not receptor-dependent. J. Biol. Chem. **280:**36657–36663.

47. **Welch, R. A.** 2001. RTX toxin structure and function: a story of numerous anomalies and few analogies in toxin biology. Curr. Top. Microbiol. Immunol. **257:**85–111.

48. **Wessel, D., and U. I. Flugge.** 1984. A method for the quantitative recovery of protein in dilute solution in the presence of detergents and lipids. Anal. Biochem. **138:**141–143.

49. **Yamamoto, N., N. Yamamoto, M. W. Petroll, H. D. Cavanagh, and J. V. Jester.** 2005. Internalization of *Pseudomonas aeruginosa* is mediated by lipid rafts in contact lens-wearing rabbit and cultured human corneal epithelial cells. Investig. Ophthalmol. Vis. Sci. **46:**1348–1355.

50. **Yates, W. D.** 1982. A review of infectious bovine rhinotracheitis, shipping fever pneumonia and viral-bacterial synergism in respiratory disease of cattle. Can. J. Comp. Med. **46:**225–263.

51. **Yuan, C., J. Furlong, P. Burgos, and L. J. Johnston.** 2002. The size of lipid rafts: an atomic force microscopy study of ganglioside GM1 domains in sphingomyelin/DOPC/cholesterol membranes. Biophys. J. **82:**2526–2535.

52. **Zacharias, D. A., J. D. Violin, A. C. Newton, and R. Y. Tsien.** 2002. Partitioning of lipid-modified monomeric GFPs into membrane microdomains of live cells. Science **296:**913–916.

Editor: D. L. Burns